

## Friction Stir Process: A Comprehensive Review on Material and Methodology

Vishal Bhojak<sup>a</sup>, Jinesh Kumar Jain<sup>a,\*</sup>, Kuldeep Kr Saxena<sup>b</sup>, Bharat Singh<sup>c</sup>, & Kahtan A Mohammed<sup>d</sup>

<sup>a</sup>Department of Mechanical Engineering, Malaviya National Institute of Technology, Jaipur 302017, India

<sup>b</sup>Division of Research and Development, Lovely Professional University, Phagwara, Jalandhar 144402, India

<sup>c</sup>Department of Mechanical Engineering, GLA University, Mathura 281406, India

<sup>d</sup>Department of Medical Physics, Hilla University College, Babylon 51001, Iraq

Received: 31 March 2022; Accepted: 22 August 2022

In recent year, advancement of the materials and processing of the material identified as research zone to make an impact in aerospace, automobile, marine and bio-medical implants application. Improvement of the material structure and surface associated with high energy requirements as well as may contain environments harmful content, like physical and chemical vapor deposition consumes high energy and extract toxic elements. Friction stir process (FSP) is surface modification and surface composites fabrication process, which works as a solid-state process. This process based on friction between the tool and workpiece which generates heat used for modification of the material. There is no fumes generation and low energy requirement, so it comes under the domain of green technology. Customized vertical milling machine is used to perform friction stir process/welding. In this review paper, an attempt has been made to study the FSP process at a glance with brief bibliometric analysis of relevant research in last two decades. Influence of the key process parameters i.e., rotational speed, traverse speed, tool geometry and machining parameters on the microstructure and mechanical properties have also been discussed. A case study on the process parameter optimization range has been done to ensure the range of parameters. This study helps to reduce the defects during the process and improve the associated properties of the processed material. Potential difficulties and the possible measures have also been suggested for giving the future direction.

**Keywords:** Bibliometric analysis, Grain refinement, Green technology, Severe plastic deformation, Surface modification

### 1 Introduction

Sustainable development is essential for meeting the growing demand of industry with essential control over the vital polluting ingredients. World organizations such as the United Nations Security Council aim to create a more sustainable world so that such problems as climate change and pollution, among others, can be addressed<sup>1</sup>. The United Nations Environment Program has set 17 Sustainable Development Goals (SDGs), with the 9th goal devoted to the implementation of sustainable development through industry, innovation, and infrastructure. It claims that building new greener infrastructures, upgrading or reconfiguring existing infrastructure systems, and leveraging the power of smart technology may drastically decrease environmental effects and catastrophe risks, as well as build resilience and boost natural resource efficiency<sup>2</sup>. To accomplish the SDGs, each country has produced a strategy for the next several years to accomplish the goals. Waste management, product recycling, reduced fuel

consumption, energy use, and natural resources are essential parts of the industry-based implementation. Innovative concepts and technological innovations have been found and applied in these area<sup>3</sup>.

In this context, Friction-based joining methods, often known as "Green welding procedures," have gained interest of researchers throughout the world since they do not use or create any ecologically dangerous chemicals, gases, or other materials<sup>4</sup>. The Friction Stir Welding (FSW) procedure, which is commonly used to connect two metallic pieces using friction, was first attempted in 1991 at "The Welding Institute" in the United Kingdom using aluminum alloys<sup>5</sup>. Some noteworthy facts include the fact that friction stir welding helps to meet sustainable development goals by reducing CO<sub>2</sub> emissions by 2400 tonnes and making the welding process greener for similar and dissimilar materials<sup>6</sup>. The successful utilisation of light-weight engineering materials, notably in the automobile, aeroplane, and marine sectors, is currently one of the key priorities of enterprises<sup>7</sup>. Aluminum, magnesium, copper, and titanium alloys show great promise as steel substitutes

\*Corresponding author (E-mail: jineshjain.mech@mmit.ac.in)

in a variety of applications. Replacing steel components with aluminium alloys in the automotive industry can significantly cut global greenhouse gas emissions. Every 2 kilogramme (Kg) of steel is replaced with 1 kg of aluminium, resulting in a CO<sub>2</sub> reduction of 10 kg during the vehicle's typical lifetime. Furthermore, a ten percent weight decrease increases fuel efficiency by 6 to 8%<sup>8</sup>.

This FSW-based technique is also used in a different material-based application, named Friction Stir Process (FSP). The term FSP and process first implemented in 1998, by R.S. Mishra and his companions for aluminum alloy-based application. Friction stir processing (FSP) in terms of experimental setup and equipment, is extremely similar to friction stir welding. The sole distinction is that friction stir welding joins pieces, whereas friction stir processing improves material qualities by microstructural alteration and grain refinement<sup>9</sup>.

Uniform dispersion, strong interfacial bonding, fine-grained structure, low porosity, low power consumption, and lower post processing are distinctive advantages of FSP. This process is more energy efficient due to application of optimum heat and less material wastage. The reduced number of parts, high processed material quality and performance, reduced material processing time and longer tool life makes this process more sustainable. Also, it reduces the environmental impact as no toxic fumes and spattering occurs. Thus, the process has evolved as an emerging green technology. Reddy *et al.* employed the FSP assistance in welding process for aluminum alloys based surface composite<sup>10</sup>. Integration of FSP in the welding process results in the development of defect free surface and eliminate the material wastage in the welding process.

In the early 2000s, many researchers used FSP to induce super plasticity, but it was later used in the manufacture of surface composites of metal. In surface composites, the basic metal's surface is transformed into a metal matrix composite (MMC)<sup>11</sup>. In metal matrix composites, the entire workpiece material is converted into the composite material; however, if the need is only to improve the material's surface, as in aerospace, marine, and automobile applications where the material's valuable properties are solely dependent on the surface, converting the entire workpiece material into the composite material becomes costly/expensive and time consuming<sup>12</sup>. A change in the material's surface is sufficient for some applications. With FSP surface composites, just

the workpiece's surface is composited; the remainder of the workpiece's material stays the same as the base material. FSP can be done with or without reinforcement, according on the requirements<sup>13</sup>. To improve the material's mechanical, tribological, and microstructural properties, researchers used different natural and synthetic reinforcement<sup>14,15</sup>. As a result, as a more environmentally friendly technology, FSW/P has grown through time and may now be used as a viable application-based process. The role of the FSP in the global scenario, as well as the contributions of nations and writers, are examined in the next section.

Friction stir mechanism based of friction between the surfaces due to which heat generation takes place without fumes generation. The researchers emphasized these techniques as a green technology or environmentally friendly processes. A series of these processes like friction stir welding, friction stir processing, friction stir riveting, friction stir spot welding, friction stir casting and research goes on, so in coming years few more advancement takes place with friction stir concept. In this literature, the friction stir process has been discussed the research in this domain from its beginning to recent time and could be in near future. There are some ways to quantify the work in particular domain or research areas, from that a brief analysis could be observed. Publication in science indexed, Scopus, based data has been analysed with some tools like web of science, dimensions, tailor and francis data set, springer data set, etc. tools able to map the work has been completed related to this field. In this work, science indexed publication in different article taken for consideration of friction stir process from 2002 to 2021 by using the web of science tool. Fig. 1, shows a significant growth of publication from 2002 to 2021 in the domain of friction stir process. Total 5901, publication identified between 2002-2021, around

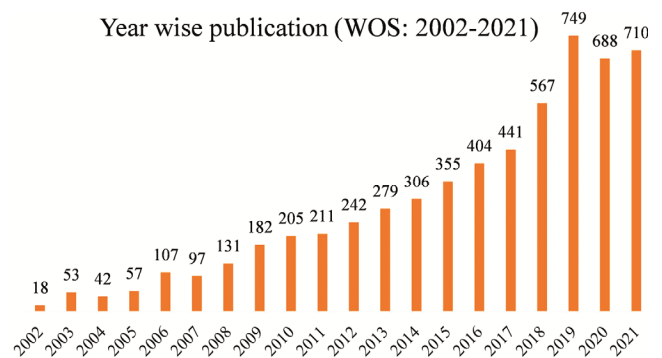


Fig. 1 — Year wise number of published papers in FSW/P from 2002 to 2021 (source: Web of science, 2002-2021).

two-decade period and the keyword for the web of science is “friction stir process”.

As per the reliable data source (web of science), the year wise publication summary of FSW/P over the world wide is displayed in Fig. 1.

A conclusion also developed during the observation; friction stir process is related to modification of surface by achieving in changes the microstructure of material. Fig. 2, shows most influential research areas which associated during friction stir process. The field of materials, metallurgy, engineering and so on; are the research work related to this domain. On behalf of that, FSP play a significant role in the research field of materials and metallurgical field which verify the number of publications related to this domain shown in figure (data have been taken from the web of science from 2002-2021).

Application like automobile, railways, marine, bioimplants, defence etc. has been described regarding the use of FSP in figure (FSP Related).The development of the process for make this process accessible to serve the common purpose or feasible. One more Fig. 3, shows the country wise contribution,

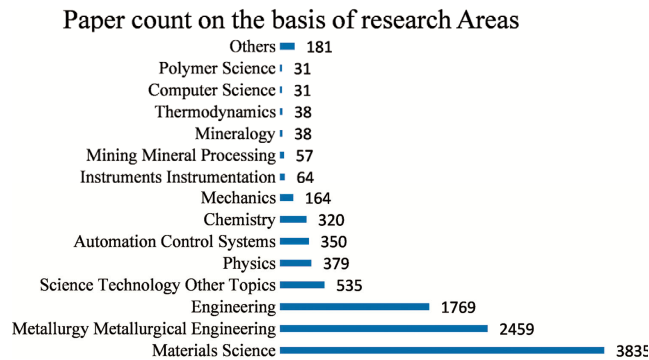


Fig. 2 — Focused research areas through friction stir process (source: Web of science, 2002-2021).

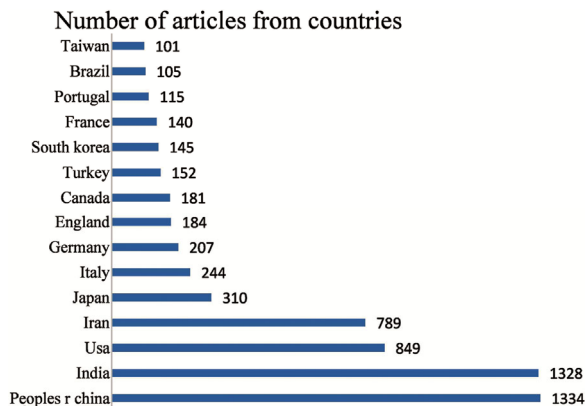


Fig. 3 — Friction Stir Welding/Process publications over world-wide (source: Web of science 2002-2021).

emphasized work in process with that nation. As FSW technique developed in UK and FSP idea come from USA, after words this technique emphasized throughout the world. In which China and India have the significant role publication in this field with 1334 and 1328 publication respectively shown in the Fig. 3. The developing countries are focused for the energy efficient process due to the limited availability of the resources. FSP is a green and energy efficient technology which can develop the industrial products with the minimum use of energy. This might be reason for focusing more research in developing nation than the developed nation. As per the reliable data source, the year wise publication summary of FSP over world-wide is displayed below given Fig. 1. It clearly indicated from the Fig. 2, the contribution of Indian author and institution during the two decades is significant. India, as country published 1328 papers out of 5901, data is taken from the web of science from 2002-2021.

The research association and institution of the nation shows the nation integrity in research direction and approach of nation regards to achieve sustainable development goals. The Indian institute of technology system and National institute of technology system of India have significant contribution in the field of friction stir process development, placed 1<sup>st</sup> with 382 publication and 2<sup>nd</sup> position with 230 publication over world-wide shown in Fig. 4(data have been taken from the web of science from 2002-2021).

Top 15, contributors throughout the world have been shown in

Fig. 5(data have been taken from the web of science from 2002-2021). Rajiv s Mishra as contributor in developing and first use of friction stir process, has first position with 146 publications in this

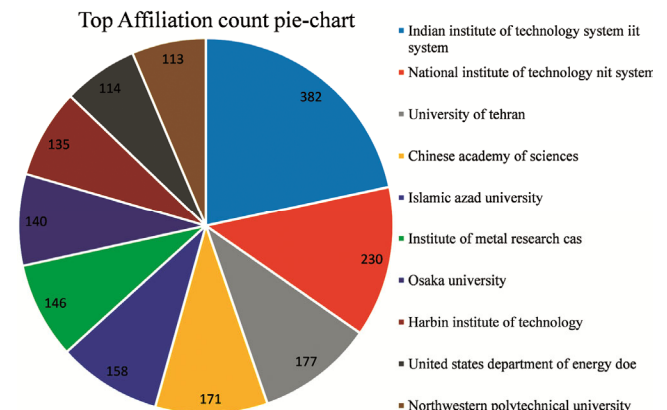


Fig. 4 — World-wise universities contribution in field of Friction Stir Process (Source: Web of science, 2002-2021).

domain. Visvalingam balasubramanium and Arshad noor siddiquee have the significant publication (in top 15) from the India and the publication count are 82 and 51 respectively.

In this section, the presence of FSP has been discussed, its application year by year increased, developing countries takes initiative to contribute in sustainable development processes, material science main research area as FSP perspective. In the further sections, the process parameters of the FSP have been discussed. The importance of parameters with the respect of material mechanical, microstructural and wear have been identified. The cause of defects during the FSP have been identified and discussed in further section. The responsible parameter for defects needs to optimize. The case study also includes to find out the optimize value and range for the individual parameter for reference. Research articles

taken as a reference to obtained the optimize range of the parameter. Also, the future importance of the FSP in material processing and product development are discussed.

## 2 Materials and Methods

The standard friction stir process setup includes a tool with both rotation and traversal speed. A downward force is imparted to the tool, as well as rotational and traversal movement(as depicted in Fig. 6). The rotating tool pin is then lowered into the workpiece until the tool shoulder makes contact with the surface<sup>16</sup>. The friction between the tool and the workpiece helps to produce enough heat in the workpiece material to cause significant plastic deformation. Due to the tool's stirring action, the workpiece material moves with the tool from the advancing side to the retreating side of the workpiece. After then, the tool is given the traverse speed, which assists in the transverse processing of the workpiece<sup>17</sup>. The method is thermomechanical in nature and assists in the significant refining of the grain size of the workpiece material. Friction stir alloying (FSA) is a form of friction stir processing that may be divided into two categories: processing without reinforcing particles and processing with reinforcing particles. Localize heat softens the work material during the process, largely due to frictional and plastic deformation via the friction stir tool, resulting in the

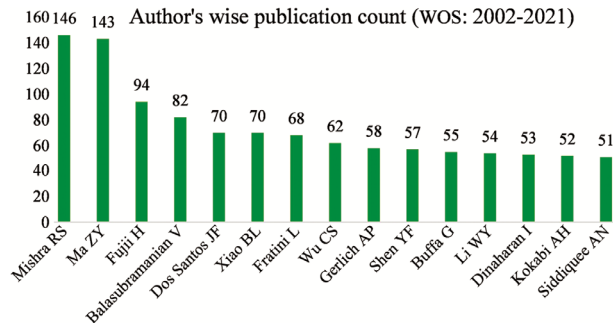


Fig. 5 — World-wise author’s contribution in field of friction stir process (source: Web of science, 2002-2021)

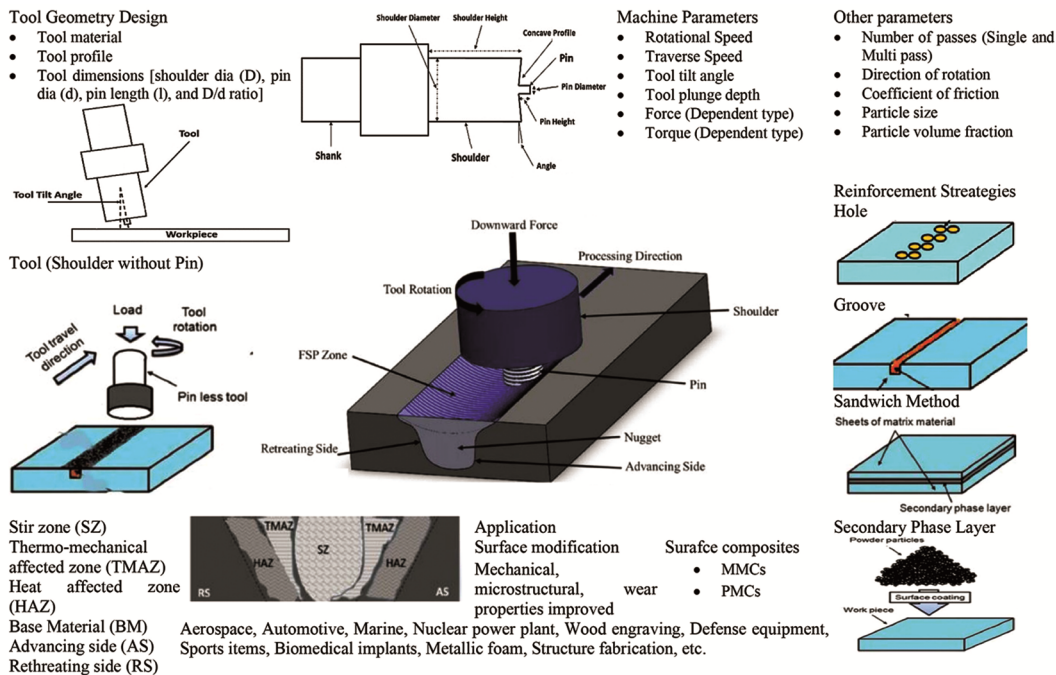


Fig. 6 — Broad schematic description of friction stir process.

production of distinct zones with inherent microstructural properties, as illustrated schematically in Fig. 6. Friction and extreme plastic deformation are principally caused by the tool's shoulder and pin, respectively. As a result, FSP may be categorised as a material processing technology that uses severe plastic deformation (SPD)<sup>18</sup>. Similar to FSW, the process temperature during FSP is controlled below the melting temperature of the work material. FSP has been shown to be effective in a range of applications, including removing casting defects (porosity), changing the microstructure of cast alloys, and creating surface composites<sup>19</sup>. The stirring action promotes grain refinement and gives the base metal extraordinary plasticity<sup>20</sup>. FSP is a technique for eliminating faults in cast and forged materials that are localised. It changes the microstructure and removes defects-causing fractures and holes. It creates equiaxed recrystallized grains, which contribute to the material's super plasticity. FSP assists in the creation of recrystallized grains, which result from the spinning activity of the tool<sup>21</sup>. In the realm of super plasticity, friction stir processing is also an essential technique. FSP has significantly improved super plasticity in a variety of Al alloys. The FSP may be used to refine grains, which improves forming and formability.

Fig. 6, depicts a comprehensive overview of FSP. This diagram depicts the basic concept of the friction stir process, in which the tool rotates from the advancing to the rethreading side. This diagram consists of broad view of friction stir process which covers a brief explanation of the whole process. In the figure the machining parameters like rotational speed, traverse speed, tool tilt angle, tool plunge angle, force and torque are mentioned. The machining parameters discuss in-depth in further section. Variables like the number of passes, rotating direction, coefficient of friction, particle size, and dispersion all have an impact on the process. As previously stated, the form of the tool is critical in terms of material flow in which tool material, tool profile and tool dimensions plays a significant role in process<sup>22</sup>. The tool geometry has been discussed in the further sections to know the effect on the processed material structure. The friction stir method is used to modify surfaces and make surface composites. For microstructure modification and secondary phase particle filling, this pin less tool is employed. The processed zone's microstructure has been classified into four zones: stir zone (SZ), thermo-mechanical affected zone (TMAZ),

heat affected zone (HAZ), and base material (BS). These zones have varied microstructures and grain alignments, which will be examined in more detail in the next section. Surface composites manufacturing evolved throughout time based on the FSP process, in which secondary particles were mixed in with the base material in a variety of ways, including hole filling, grooves, sandwich methods, and secondary phase layers, as illustrated in Fig. 6<sup>23</sup>. Aerospace, automotive, maritime, nuclear power plant, wood engraving, defence equipment, sports goods, biomedical implants, metallic foam, structure fabrication, and other real-world applications of FSP are shown in this diagram. The flow creation during the friction stir process has been studied and described with graphic representation in the following subsection of the friction stir process (shown in Fig. 7)<sup>24</sup>.

Flow pattern of material during FSP in diagram (Fig. 7) clearly shows the mechanically stirred zone (SZ). The white line demarcates the edge of the stir zone. During the FSP, it denotes the complete development of the SZ and the continuous flow of plasticized material. Frictional heat is created by rubbing the tool shoulder and shearing the pin, which plasticizes the material surrounding and below the tool<sup>25</sup>. The material beneath the tool is forged inwards, creating a hollow on the advancing side. As the tool advances, material flows from the retreating side to the advancing side. The distorted material is put at the retreating side behind the tool. Within the pin diameter, the material is forced lower on the advancing side and moved higher on the retreating side<sup>26</sup>. Fig. 7, shows that the SZ region is free of defects such as pinholes, wormholes, and tunnels.

During FSP, the microstructure changes due to thermal-mechanical reactions. Similar to FSW, FSP's processing zone is divided into a stir zone (SZ), thermomechanical affected zone (TMAZ), heat-

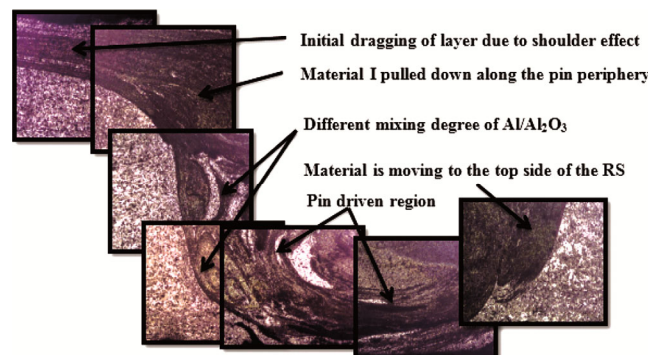


Fig. 7 — Material flow during the fabrication process<sup>33</sup>.

affected zone (HAZ), and base metal zone (BM). When compared to the base metal, the SZ is largely made up of homogeneous refined equiaxed grains<sup>27</sup>. During the FSP process, SZ is exposed to a high peak temperature and considerable plastic deformation, resulting in microstructure change due to dynamic recrystallization. The proportion of high-angle grain boundaries (HAGBs) in the processing zone rises after FSP, promoting grain boundary slippage and a notable increase in the flexibility of the base metal<sup>28</sup>.

In stir zone an onion ring pattern produces as the plastic material layer moves from the front to the rear of the tool<sup>29</sup>. This can be used to describe the flow of the material. In the TMAZ, grain deformation and partial recrystallization are caused by thermal cycling and mechanical stirring. The precipitate phase looks to be disintegrating in this site<sup>30</sup>. When reinforcing particles are added to the metal matrix, particle-stimulated nucleation favours the creation of grains during recrystallization<sup>31</sup>. According to the Zener–Holloman mechanism, the equally dispersed small particles can prevent grit formation during the dynamic recrystallization process. This is done by pinning grain boundaries, which results in significant microstructure refinement<sup>32</sup>.

To summarise, the material flow during FSW/P is complicated, and our understanding of the deformation process is restricted. It's important to remember that the material flow during FSW/P might be altered by a number of factors. Material types, workpiece temperature, and so on. Tool geometry (pin and shoulder design, pin and shoulder relative dimensions), welding parameters (tool rotation rate and direction, i.e., clockwise or counter-clockwise, traverse speed, plunge depth, spindle angle)<sup>34</sup>. The material movement within the nugget during FSW/P is most likely made up of many discrete deformation events.

Friction stir process is green process which improve the surface structure and fabricates the surface composite. The brief scenario of the application and research on this process has been discussed in the introduction part. The friction plays an important aspect during the FSP/W. The FSP is performed over the vertical milling machine with customize setup, in which process parameters calibrated according to the material. To make the product defects free, it is important to know about the process parameters and their role in the flow mechanism and heat generation over the processed zone. In further section, important process parameters discussed in the detail with their impact on the

properties of the material. Experimental as well as review articles from the different journals taken in to consider for the study of the behaviour analysis. Later on in the article, an optimization range has been identified and establish the importance of parameters to reduce defects during the process. Research gaps are identified and concluded as future scope in the article.

### 3 Results and Discussions

Small processed area routes, homogeneity, and precise microstructures, as well as densification, have all been demonstrated using FSP. Processing parameters such as rotational speed, travel speed, plunge rate, heat input, and cooling/heating methods, as well as tool geometry such as shoulder diameter, probe length, probe profile, groove dimensions (width and depth), have all been found to be effective in controlling the mechanical and metallurgical properties of the processed zone in studies. Fig. 6 displays different process parameters that influence the FSP and is broken down into sections.

#### 3.1 Friction stir process parameters

Multi-pass: Single-pass FSP enables for surface texture modifications because only one tool passes the supplied region. The tool is traversed in the same or opposite direction over the complete (or a pre-set proportion) of the previously processed region in multi-pass FSP<sup>35</sup>. Multi-pass FSP can yield more grain size reduction and texture deterioration than single-pass FSP due to cumulative strain rates induced by multiple runs<sup>36</sup>. It also increases the homogeneity of grain dispersion in the material. It has the capacity to reduce the occurrence of tunnel faults in the agitated region<sup>37</sup>. The effects of multi-pass FSP on the microstructure, microhardness, and tensile strength of metal alloys and composites have been studied by a number of researchers<sup>38</sup>. The application of multi-pass FSP in die casting Al-7Si-3Cu aluminium alloy was investigated by Baruch *et al.*<sup>39</sup>. The number of overlapping passes FSP resulted in significant refinement and dispersion of the silicon eutectic phase, as well as lower casting porosities. As the number of passes increases, microstructure refinement occurs, resulting in improved ultimate tensile strength and ductility as fracture strain increases<sup>40</sup>.

Force and torque in FSP: The most essential loads acting on a machine during the FSP (FSW) process are axial force ( $F_z$ ), traverse force ( $F_x$ ), side force ( $F_y$ ), and torque ( $M$ ). Because of its rotational and linear (curvilinear) movements, the tool exerts axial and

transverse stresses on the changed material in the FSP and FSW processes. These forces can result in tool wear, altered element deformation, and clamping system deformation. As a result, forecasting, monitoring, and managing these forces and torques is crucial<sup>41</sup>. Understanding the aforementioned phenomena aids in improving tool design, estimating tool wear, improving clamping systems, predicting needed clamp pressures, improving the quality of the altered surface, and selecting the optimal FSP (FSW) machine. The forces and torque operating on the FSP (FSW) tool can be measured using a variety of ways. To measure axial and transverse forces, as well as torque, one of two approaches can be utilised. Strain gauges, load cells, and dynamometers are examples of direct measuring instruments. During the FSP (FSW) process, however, monitoring the current or power of the driving motor is an indirect measurement approach<sup>42</sup>.

Arora *et al.*<sup>43</sup> findings on the relationship between parameters and  $F_x$  force were given. The  $F_x$  force grew as the rotation speed, shoulder diameter, and pin diameter increased, while the force reduced as the travelling speed increased. On the other hand, spindle torque is one of the most essential quantitative elements that effects heat input, stir zone temperature, clamping system, and machine safe load. In most cases, the total of the sticking and sliding torques equals the torque. The overall torque increases despite the fact that the sticking torque decreases as the shoulder diameter grows. In this regime, the decrease in sticking torque is less than the increase in sliding torque<sup>44</sup>. As a result, as the shoulder's diameter increases, so does the entire torque. At various rotating speeds, a variety of behaviours can be seen. The torque diminishes when the speed is raised. This is because the temperature of the surface between the shoulder and the altered material, as well as the stir zone, rises as the tool's spinning speed increases. As the friction coefficient decreases, the material resistance decreases. Plastic deformation is also a possibility when the material is altered<sup>45</sup>. The torque loss might be due to one of two factors. For starters, a constant tool rotation speed combined with a slower travel speed minimises the amount of material deformed every revolution, resulting in less heat being generated in a smaller volume, potentially leading to higher temperatures and less flow stress. Second, reduced travel speeds will minimise convective cooling because of the delayed transit into

the somewhat cooler material in front of the tool. The spinning speed of the FSP tool has a significant impact on spindle torque<sup>46</sup>. The friction coefficient lowers when the temperature in the FSP area (modified material) rises as the rotating speed increases. It's worth noting that the down force was nearly constant throughout the research, with just tiny variations<sup>47</sup>.

Tool rotational speed: Another important processing parameter that determines the degree of plasticity and material flow that may be achieved in the treated material is the rotation speed. The tool rotation speed regulates the kind of microstructure creation in friction stir processing, which impacts the properties of the treated material<sup>48</sup>. The tool rotation speed affects the degree of grain refining. The spinning speed must be raised when a higher temperature is required, resulting in larger grain sizes. When the rotation rate to traversal speed ratio increased, the grain size and proportion of high-angle grain boundaries (HAGBs) increased as well<sup>49</sup>. The maximum rotating speed in the stir zone induces metallurgical transformations such as solubilization, re-precipitation, and coarsening of strengthening precipitates, as well as a reduction in dislocation density, which lowers tensile strength and % elongation. The material's microstructure can be controlled by changing the spinning speed<sup>50</sup>. The rotation speed had a considerable impact on the coefficient of friction of the specimen. Because of the extreme plastic deformation and impacted cooling rate by the tool's travel speed, fine equiaxed grains are created by tool rotation paired with the correct tool transverse speed<sup>51</sup>. The tool velocity ratio, which is the ratio of the tool's rotation speed to its traverse speed, was observed by p. vijayavel *et al.*<sup>52</sup>. A ratio of 2.6 is recommended for a defect-free and homogeneous stir zone profile. This is the ratio that takes both rotational and traversal speeds into consideration. As the rotational-to-travel speed ratio grows, heat input and plastic deformation increase, resulting in more homogeneous nanoparticle dispersion. The area of the surface composite rises as the tool rotates faster<sup>53</sup>.

Traverse speed: Increased transit speed can result in less heat input, resulting in insufficient material flow to scatter particulates<sup>54</sup>. The material's changing characteristics are influenced by the interaction of the tool's transverse and rotational speeds<sup>55</sup>. Due to a typical combination of transverse and rotational speeds, with lower rotational speed and higher traverse speed, the treated material exhibited a higher

microhardness<sup>52</sup>. The proper blend of these two processing factors must be set to achieve the required microstructure and, as a consequence, the desired features. The coefficient of friction decreased from 0.4 to 0.07 as the tool travel speed increased. The tool's wear resistance increased when the tool's travel speed was increased<sup>56</sup>. The increased travel speed is projected to be too fast to provide enough heat flow in the AZ91 matrix to allow MWCNT dispersion at constant rotation speed<sup>57</sup>. Table 1, summarises the effect of rotational and traversal speeds on the parameters of processed FSPed material.

**Tool tilt angle:** Tool tilt improves tool life by decreasing tool thrust, and it may also be used to repair faults such pin holes, cavity expansion, and tunnel type defects when compared to 0° tilt. Increased tool tilt angle causes proper material consolidation behind the shoulder, and non-circular tool profiles result in a worked microstructure with high ductility. As the tilt angle increases, so does the yield strength. The material compaction increases as the tilt angle rises, resulting in increased yield strength. The FSP tool is tilted away from vertical by a few degrees to maximise forging action<sup>44</sup>.

**Tool plunge depth:** Plunge depth is the distance between the tool shoulder's lowest point and the

welded plate's surface, and it may also refer to the contact between the tool shoulder and the work piece. The depth of the dive has been revealed to be an important factor in heat generation and defect-free material consolidation<sup>58</sup>. The amount of force required during the plunging technique is determined by the depth of the dive. When the plunge depth was increased, the rate of deterioration was demonstrated to be lowered. This might be due to the water hardening when the diving depth is raised. The penetration diminishes when the rotation speed is raised owing to a rise in temperature inside the stir zone.

**Tool Geometry:** The processing tool is renowned for two main functions: heating the workpiece material and deforming it with proper mixing. The tool shape is another important aspect of friction stir processing. The researchers looked at several tool geometries and concluded that they had a big impact on the characteristics obtained during friction stir processing. This solid-state joining method employs a spinning tool with a shoulder and/or a probe<sup>59</sup>. The shoulder presses down on the workpiece surface, restricting the plasticized material around the probe, creating heat through friction, and increasing plastic deformation beneath the bottom surface of the shoulder. The rotating probe drags the material in the

Table 1 — Effect of rotational and traverse speed

Process parameters	Material Properties	Inference
Rotational Speed	Hardness	Hardness of the stir zone increases when the rotational speed increases, because grain refinement takes place. But after certain limit, if rotational speed increases the hardness started reducing because higher heat generation takes place <sup>62</sup>
	Tensile strength	The ultimate tensile strength improved comparatively base material, due to grain refinement takes place <sup>63</sup>
	Grain refinement	The higher the tool rotates, the faster the grains break up and the mechanical intermixing of the particles increases. As a result, grains are distributed more finely and uniformly <sup>64</sup>
	Wear rate	The hardness of the grain will grow when it is refined. The material's wear rate reduces as the hardness value rises. As a result, the rate of wear is inversely related to the hardness of the material <sup>65</sup>
	Damping capacity	At low rotational speed, damping capacity of the processed material is good as compare to high rotational speed. The grain structure will be fine as compare to high rotational speed processed material. Due to which no of grain boundaries more which contribute to transfer energy as compare to coarse grain structure material <sup>66</sup>
Traverse Speed	Hardness	As the traverse speed is reduced, the SZ's hardness improves as the grain refinement improves. Higher traverse enhances hardness in surface composites owing to particle aggregation <sup>33</sup>
	Tensile strength	Tensile strength of the FSPed material improved compare to lower traverse speed rather higher rotational speed <sup>67</sup>
	Grain refinement	Grain size decreases as traversal speed increases. Increased traverse speed reduces heat input to a region and reduces the time that that region is exposed to high temperatures. As a result, the amount of time available for grain growth is limited, resulting in grain size reduction <sup>68</sup>
	Wear rate	When the traverse speed is reduced, the wear rate drops. Wear is a surface phenomenon that is linked to the surface's hardness. Low wear of the material was noticed when the hardness of the material improved with decreasing traverse speed <sup>69</sup>

stir zone along with it, plasticizes it, and mixes it, resulting in a non-fusion junction. The heat generated by the shoulder accounts for 75% of total heat generation<sup>60</sup>. Due to tool rotation and translation, the material goes from the front to the rear of the probe. Significant obstacles, such as tool design and wear, have restricted FSW/ P's adoption in production, particularly for alloys with high melting temperatures or high strength<sup>61</sup>. The tool types, shapes, dimensions, materials, and wear characteristics of FSP tools are briefly summarised in this article.

Fixed, adjustable, and self-reaching FSP tools are the three categories. The fixed probe tool's shoulder and probe are both made of a single piece. Due to the set probe length, this equipment can only fuse a workpiece of a particular thickness. The entire gadget must be replaced if the probe wears out or breaks. The instrument is made up of two parts: a shoulder and a probe that may be changed for probe length during the FSW/P procedure<sup>70</sup>. The shoulder and probe of this design may be made out of a variety of materials, and the probe can be simply replaced as it wears out or breaks<sup>71</sup>. The upper shoulder, probe, and lower shoulder make up a bobbin type device. Because of the changeable probe length between the top and bottom shoulders, this instrument can support a broad variety of gauge thickness joints<sup>72</sup>. There are two sorts of tool shapes: shoulder and probe.

**Shoulder shapes:** Tool shoulders are designed to heat the workpiece's surface regions, provide the necessary downward forging action for welding/ processing consolidation, and keep hot metal contained beneath the bottom shoulder surface<sup>73</sup>. Fig. 8 summarises the normal shoulder outer surfaces, bottom end surfaces, and end features. The shoulder's outer surface is usually cylindrical, but it can also be conical. A flat shoulder end surface is the most basic shape<sup>74</sup>. The flat shoulder end surface is inadequate in

trapping flowing metal material under the bottom shoulder as a result of its design, resulting in increased material flash<sup>75</sup>. For this reason, a concave shoulder end surface was created, and it is now commonly used to avoid material extrusion from the sides of the shoulder<sup>76</sup>. Tool shoulders are designed to both heat and support the workpiece's surface regions. As the tool travels ahead, the concave shape gives forging action to the material below, causing the material to be pushed behind. For best shoulder performance, the tool should be tilted 1–3° away from the normal of the workpiece and in the opposite direction of motion<sup>77</sup>. This is necessary in order to maintain the material reservoir full while applying a compressive forging force to the weld using the shoulder tool's trailing edge. Higher forging and hydrostatic pressures might lead to more material churning and better nugget integrity<sup>78</sup>.

Another option for shoulder endings is a convex profile. Although the convex shoulder profile's main advantage is that it can make contact with the workpiece anywhere along the convex end surface, accommodating differences in flatness or thickness between the two adjoining workpieces, the smooth end surface's inability to prevent material displacement away from the probe is a disadvantage. Several features on the shoulder end surfaces may be used to increase workpiece mixing and surface quality by promoting material friction, shear, and deformation<sup>80</sup>. As seen in Fig. 8, popular shoulder end designs include flat (smooth or featureless), scrolls, grooves, and concentric circles. Scrolls are the most prevalent shoulder feature.

**Probe shapes:** The friction stirring probe may be used to achieve frictional and deformational heating. Theoretically, it should disturb the workpiece's contacting surfaces, shear the material in front of the tool, and transfer the material behind the tool. The bulk of the deformation depth and tool travel speed are determined by the probe<sup>81</sup>. The terminal shape of the probe is either flat or domed. The flat bottom probe is the most popular probe design, which emphasises ease of fabrication. The huge forging force required when diving is the flat probe's most serious defect. A round or domed end form, on the other hand, may minimise forging force and tool wear during plunging, increase the quality of the processed root at the probe's bottom, and extend tool life by reducing local stress concentration. These benefits appear to be greatest when the dome radius is 75 percent of the probe diameter<sup>82</sup>. The local surface velocity and the friction coefficient between the probe and the metal dictate the deformation during friction stirring. Raise the surface

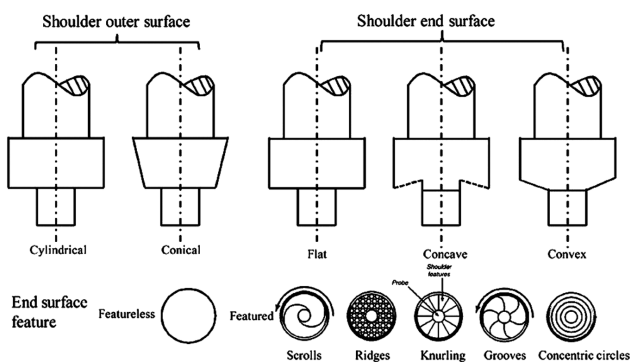


Fig. 8 — Tool shoulder shapes of outer surface profile and end surface features<sup>79</sup>.

velocity at the probe's edge, which enhances metal flow beneath the probe end, to boost the probe's stirring power. Although the exterior surface of the FSW/P probe is normally cylindrical, a tapered outer form, as illustrated in Fig. 9, can also be used<sup>83</sup>. The frictional heat induces more plastic deformation because the probe has a bigger contact area with the workpiece with the tapered probe. In the nugget zone, the tapered probe also maintains a high hydrostatic pressure, which is crucial for increased material stirring and nugget integrity. On the other side, high heat and hydrostatic pressure can result in substantial tool wear<sup>84</sup>.

Threads, flats, and flutes can be found on the probe's exterior surfaces. Because threaded features

may wear away fast in high-strength or highly abrasive metals, threadless probes are utilised instead of threaded probes<sup>85</sup>. It has been demonstrated that adding flat features to a probe changes the way material moves around it. This is owing to the flats, which act as paddles, causing local deformation and turbulent flow in the plasticized material. TWI developed Whorl and MX Tri flute tools for welding Al alloys up to 50–60 mm thick<sup>86</sup>.

A schematic representation of a tool with a shoulder and a pin is shown in Figure 10.

Fig. 10. The various aspects of the pin and shoulder have been categorised accordingly, and the tool has been quickly presented through the graphical depiction.

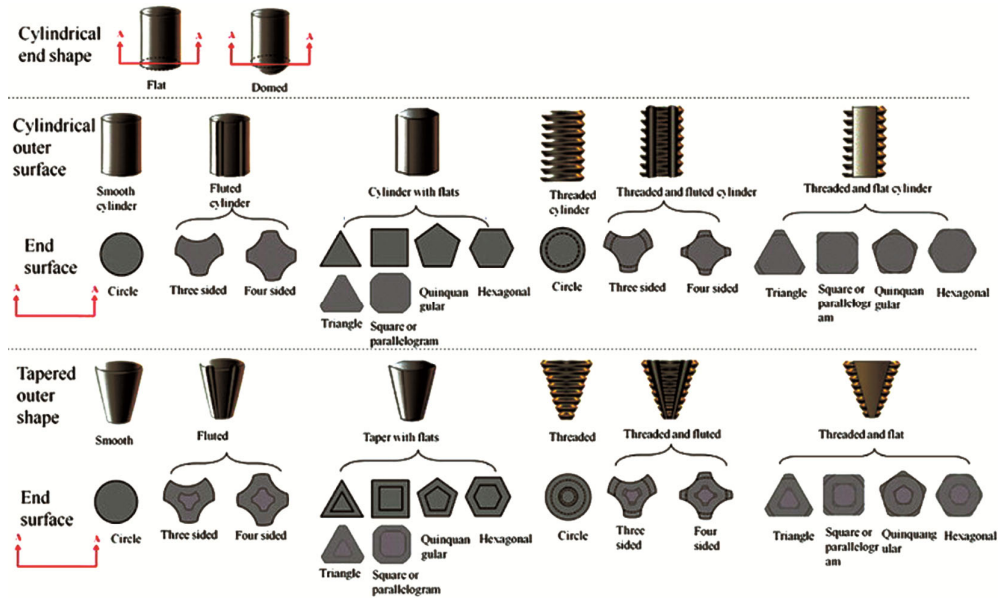


Fig. 9 — Tool pin profiles and its end surface features<sup>79</sup>.

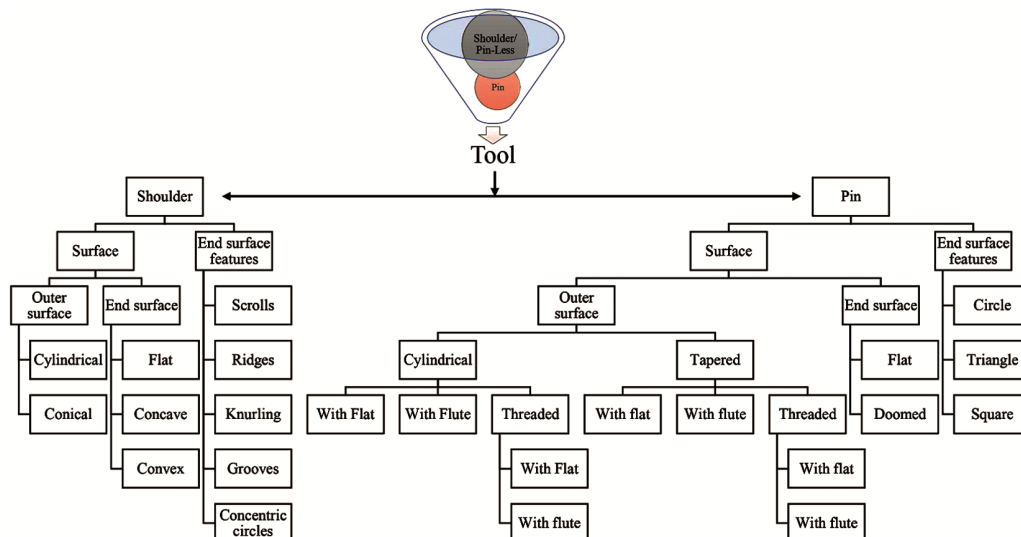


Fig. 10 — Geometric description of tool shapes and its features tool materials.

Tool material properties may be critical for FSW/P. The projected tool material is influenced by the workpiece material and expected tool life, as well as the user's own experiences and preferences. Thermal cycling of heating and cooling during workpiece processing causes compressive yield stresses, higher forging forces, thermal stresses, and fatigue in tools<sup>87</sup>. Strong tensile and compressive strength, dimensional stability, thermal fatigue resistance, creep resistance, and no harmful interactions with the workpiece's material are all requirements for the tool's material. Tool steel has a low wear rate and is often used in light metal welding/processing tools, such as those for Al, Cu and Mg alloys. Materials with a high melting point, such as titanium, nickel, steels, and other alloys, are not suitable for steel tools<sup>88</sup>. Welding/processing tools for these high-strength materials include hard metals, carbides, and metal matrix composites with improved thermal and wear endurance at temperatures higher than 1000 °C, such as WC-Co, TiC, and PCBN. As a consequence of numerous experimental investigations, several tool materials have been identified, as shown in the Table 2, below.

**Tool Wear:** The change of the shape and dimensions up to certain limits comes under wear of the tool. Due to excessive tool wear surface quality more prone to defects and final properties reduced. The wear of the tool takes place due to contact of reinforce particle, work as abrasive particle over the tool surface<sup>89</sup>. During the flow of the material and stirring of the pin, tool faces stresses and forces retard the tool motion. It can be concluded at low tool rotation speed, adhesive wear (due to which scoring, galling, or seizing takes place) is the predominant source of wear, whereas at high tool rotation rates, abrasive wear is the primary cause of wear (due to abrasive particle contact with tool surface).

Surprisingly, the self-optimized form (worn tool) without threads produced welds with no visible tool

wear. Understanding and managing the material flow associated with the probe profile in the solid state is critical for reducing tool wear and enhancing tool life<sup>90</sup>. To date, low-cost, long-life welding and processing equipment for low-strength materials such as aluminium and magnesium alloys has been well developed. Long-lasting abrasive materials tools are still absent, such as particle reinforced metal matrix composites and high-strength materials like Ti, Ni, steels, and others<sup>91</sup>. The tool's life can be extended by coating it as well as parameters discussed earlier need to optimize according to tool design.

**Secondary particle reinforcement:** Many researchers discovered that reinforcements were important in modifying the structural surface and texture of reinforced metal matrix composite materials, as well as how they enriched the materials' electrochemical, mechanical, and metallurgical properties by inducing intense, localised plastic deformation when compared to the base material<sup>92</sup>. The reviews based on composite manufacturing utilising FSP were provided by Sharma *et al.*<sup>93</sup>, Gangil *et al.*<sup>94</sup>, Bharti *et al.*<sup>95</sup>, Patel *et al.*<sup>12</sup>, and Rathee *et al.*<sup>96</sup>.

Aside from friction stir processing, additional methods for manufacturing MMCs include stir casting, powder metallurgy, squeeze casting, and compo casting<sup>97</sup>. MMCs reinforced with organic and inorganic particles in macro, micro, and nanoparticles have been made using all of these techniques<sup>98</sup>. Since the first emergence of FSP, several types of reinforcement have been used. The most often used reinforcing materials during FSP have been demonstrated to be copper, graphite, iron, silicon carbide, nitrides, WC, titanium alloy, TiB<sub>2</sub>, graphene, stainless steel, oxides such as SiO<sub>2</sub>, Al<sub>2</sub>O<sub>3</sub>, and others. Fly ash, palm kernel shell ash, coconut shell ash, rice husk, and other organic powders have also been examined.

To produce homogeneous particle distribution, secondary particles or reinforcement are filled with base material utilising holes, grooves, sandwiches, and a secondary phase layer over the base material (shown in Fig. 6). The hole method comprises drilling a series of holes into the workpiece's surface to the depth required by the surface composite. In the groove approach, on the other hand, a traverse direction groove with the required depth is used<sup>99</sup>. After that, the reinforcement is introduced into holes and grooves, and the workpiece is packed with it using a pin less tool<sup>93</sup>. The surface composite is then

Table 2 — Identified tool materials for FSP

Base materials	Tool materials used
Aluminum alloys	Tool steel (SKD61, H13, MP 159, HCHCr steel), WC-Co, MP 159
Magnesium alloys	Tool steel, WC
Copper and copper alloys	Nickel, PCBN, Tungsten
Titanium alloys	Tungsten alloys, PCBN
Stain-less steel	PCBN, tungsten alloys
Low-alloy steel	WC, PCBN
Nickel alloys	PCBN

created by inserting the tool with pin into the workpiece<sup>100</sup>. When compared to the groove method, the holes method generated a more even distribution of reinforcing particles and enabled for more powder to be added during FSP with less powder dispersion. The multi-pass and change in pass direction after each pass, in addition to the other factors, played a vital role in uniform particle dispersion and effective hybrid surface composite manufacture<sup>101</sup>.

Aluminium metal matrix composites are made by incorporating reinforcements into pure aluminium (Al-MMCs). Al-MMC reinforcement has helped to alleviate a number of flaws in pure aluminium. At a reasonable cost, the mechanical, metallurgical, and electrochemical properties of Al-MMCs with reinforcements have been considerably improved<sup>102</sup>. It was discovered that adding reinforcements to Al-MMC materials improved the ductility of the composites while also increasing their modulus and strength<sup>103</sup>. GNP is employed as a particle in the PM and FSP synthesis of Al metal matrix composites. After FSP, the mechanical and microstructure characterisation were accomplished. The GNP were broken as a result of the FSP, and the adhesion between the GNP and the Al matrix was enhanced, resulting in a considerable increase in hardness and tensile properties. Strong impact and wear resistance, low density, high melting point, high hardness, and exceptional thermal and electrical conductivity are only a few of B<sub>4</sub>C's physical and mechanical qualities<sup>104</sup>. The hardness

values of the B<sub>4</sub>C-reinforced composite are clearly greater than those of Al<sub>2</sub>O<sub>3</sub> and SiC-reinforced composites<sup>105</sup>. This is owing to the B<sub>4</sub>C particles' smaller particle size and higher intrinsic toughness. Al-B<sub>4</sub>C composites have a unique capacity to absorb thermal neutrons and are now employed in the nuclear industry as the primary neutron shielding material. Ceramic particles, on the other hand, drastically reduce the ductility and hardness of AMCs<sup>106</sup>. Because it would swiftly fail under external load, this flaw poses major safety issues. Another technique to increase AMC ductility is to reinforce them with hard, high-melting-point metallic particles<sup>88</sup>. To increase ductility, hard metallic particles might be employed as reinforcement. AMCs can be strengthened with metal particles such as nickel, copper, titanium, iron, and tungsten to increase ductility and strength<sup>107</sup>. To reinforce AMCs without losing their ductility, a variety of metal particles can be used.

The summarized contribution of the FSP parameters into different surface composites fabrication has been shown in Table 3. In Table 3, different metals and reinforce materials processed through FSP, represented. The method for reinforcing the different reinforcement with base material was groove filling commonly, for better uniformity. Different parameters have been tabulated for different combination of the metal matrix surface composites. Here some representation for parameters is described which used in the table.

Table 3 — FSP processed composites with fabrication method and range of parameters

Material system	Method of secondary phase introduction	Grain refinement (in $\mu\text{m}$ )	Parameters	Remarks
AZ31/MWCNTs <sup>108</sup>	Groove filling	Up to 0.5	r = 1500 t = 25 to 100 p = single d = 12 d <sub>0</sub> = 4 l = 1.8 Angle = 3°	<ul style="list-style-type: none"> <li>MWCNTs is hard particle, by addition of MECNTs in AZ31 Mg alloy hardness improved.</li> <li>Friction stir process refines the grain size of MWCNTs.</li> <li>At lower travel speed, uniformity of MWCNTs is comparatively better.</li> </ul>
AZ61/amorphous SiO <sub>2</sub> <sup>109</sup>	Groove filling and covering	Up to 0.8	r = 800 t = 45 p = 4 d = 18 d <sub>0</sub> = 6 l = 6 Angle = 2°	<ul style="list-style-type: none"> <li>SiO<sub>2</sub> added with AZ61 by using friction stir process. Uniform distribution of SiO<sub>2</sub> observed as number of passes increases.</li> <li>MgO and Mg<sub>2</sub>Si particles presented in the formed matrix due to friction stir process which improve properties of alloy.</li> </ul>

(Contd.)

Table 4 — FSP processed composites with fabrication method and range of parameters (*Contd.*)

Material system	Method of secondary phase introduction	Grain refinement (in $\mu\text{m}$ )	Parameters	Remarks
Thixoformed AZ91/SiC <sup>110</sup>	Groove filling	120 to 3.1	r = 450 t = 60 p = 4 d = 20 d <sub>0</sub> = 7 l = 5 Angle = 3°	<ul style="list-style-type: none"> <li>In this article the tribological behavior of the SiC reinforced AZ91 observed.</li> <li>By using FSP, SiC uniformly distributed throughout the matrix.</li> <li>SiC improve hardness of the matrix and wear properties improved.</li> </ul>
AZ91/SiC <sup>111</sup>	Groove filling and covering	150 to 0.6	r = 710 to 1400 t = 12.5 to 63 p = 8 d = 15 d <sub>0</sub> = 3.54 * 3.54 l = 2.5 Angle = 3°	<ul style="list-style-type: none"> <li>Rotational speeds influence observed and at higher speed grain size increased and microhardness decreases.</li> <li>Grain size reduces as traverse speed increases and simultaneously improved microhardness.</li> <li>The direction of the rotational speed impact on the grain structure and hardness of composite.</li> </ul>
AZ91/SiC, AZ91/Al <sub>2</sub> O <sub>3</sub> <sup>112</sup>	Groove filling and covering	150 to 1.8	r = 900 t = 63 p = 8 d = 15 d <sub>0</sub> = 3.54 * 3.54 l = 2.5 Angle = 3°	<ul style="list-style-type: none"> <li>SiC and Al<sub>2</sub>O<sub>3</sub> particles addition in AZ91 observed. It is found that the composite with SiC had improved grain size, hardness increases, strength improved, elongation enhanced and wear resistance more compare to Al<sub>2</sub>O<sub>3</sub> reinforced composites.</li> </ul>
AZ91/SiC <sup>113</sup>	Groove filling and covering	150 to 5	r = 710 to 1400 t = 12.5 to 63 p = 2 d = 15 d <sub>0</sub> = 3.54 l = 2.5 Angle = 3°	<ul style="list-style-type: none"> <li>Nano and micro size of the SiC particles observed in the composites.</li> <li>Nano particle size SiC more uniformly distributed comparatively micro sized particle.</li> </ul>
AZ31/Al <sub>2</sub> O <sub>3</sub> <sup>114</sup>	Groove filling and covering	70 to 2.9–4.4	r = 800, 1000 and 1200 t = 45 p = 4 d = 18 d <sub>0</sub> = 6 l = 5.7 Angle = 2°	<ul style="list-style-type: none"> <li>The effect of Al<sub>2</sub>O<sub>3</sub> particles in AZ31 observed by using FSP process.</li> <li>The tool used as threaded pin which improved material flow during process.</li> </ul>
AZ91/Al <sub>2</sub> O <sub>3</sub> <sup>115</sup>	Groove filling	150 to 2.8	r = 900, 1100 and 1200 t = 40, 50, 63 and 80 p = 4 d = 15 d <sub>0</sub> = 5 l = 1.8 Angle = 2°	<ul style="list-style-type: none"> <li>Nano sized Al<sub>2</sub>O<sub>3</sub> particles added with AZ91 matrix to fabricate composites using FSP.</li> <li>The number of passes effect study identified as uniform grain structure throughout composites.</li> </ul>
AZ31/SiC <sup>116</sup>	Direct supply through the FSP tool	to 1.24	r = 710 to 1400 t = 12.5 to 63 p = 1 d = 15 d <sub>0</sub> = 3.54 * 3.54 l = 2.5 Angle = 3°	<ul style="list-style-type: none"> <li>Particles introduced in the composites using direct friction stir processing (DFSP).</li> <li>DFSP composites compared with FSP fabricated composites and better grain refinement found in DFSP made composites.</li> </ul>

*(Contd.)*

Table 5 — FSP processed composites with fabrication method and range of parameters ( <i>Contd.</i> )				
Material system	Method of secondary phase introduction	Grain refinement (in $\mu\text{m}$ )	Parameters	Remarks
AZ31/nano-SiC <sup>117</sup>	Groove filling	Up to 1	r = 1000 t = 15 p = 1 d = 16 d <sub>0</sub> = 5 l = 2.6 Angle = 2°	<ul style="list-style-type: none"> <li>• Hardness of the composites improved by using nano SiC particles observed.</li> <li>• Nano-SiC forms the SiO<sub>2</sub> particles, which improved the hardness of the composites.</li> </ul>
AZ31/nano-hydroxyapatite <sup>118</sup>	Groove filling	1500 to 3.5	p = 1 tapered 5 to 3 mm l = 5 Angle = 2°	<ul style="list-style-type: none"> <li>• Nano hydroxyapatite added with AZ31 by groove filling method. Biodegradable Composites fabrication for implants application.</li> <li>• Immersion test performed to check bioactivity.</li> <li>• Bioactivity improved and deterioration of the sample decreases.</li> </ul>
Mg/nano-hydroxyapatite <sup>16</sup>	Groove filling	56 to 2	r = 1200 t = 12 p = 1 d = 15 d <sub>0</sub> = 3 to 5 l = 2.7 Angle = 3°	<ul style="list-style-type: none"> <li>• Nano-hydroxyapatite addition improved the cell adhesion properties.</li> </ul>
AZ31/TiC <sup>119</sup>	Groove filling and covering	Not reported	r = 1200 t = 40 p = 1 d = 18 d <sub>0</sub> = 6 l = 5	<ul style="list-style-type: none"> <li>• The bonding between TiC and Mg particles improved using FSP. TiC uniformly distributed by using optimised FSP parameters.</li> </ul>
AZ91/SiC <sup>116</sup>	Groove filling and covering	150 to 7.1	r = 710 to 1400 t = 12.5 to 80 p = 1 d = 15 d <sub>0</sub> = 3.54 * 3.54 l = 2.5 Angle = 2.5°, 3°, 3.5°, 4°	<ul style="list-style-type: none"> <li>• Effect of different angle had been observed and requirement of force during process reduced.</li> </ul>
AZ91/Al <sub>2</sub> O <sub>3</sub> <sup>120</sup>	Groove filling	130 to 6	r = 500 to 2000 t = 20, 40 and 80 p = 1 d = 15 d <sub>0</sub> = 4.5 l = 4.5 Angle = 3°	<ul style="list-style-type: none"> <li>• Shape of the tool pin effect observed during FSP. compare to circular pin, square pin distribute particle uniformly.</li> </ul>
Commercial - Al <sup>121</sup>	Hole filling and covering	500 to 3	r = 1180 t = 60 d = 16 d <sub>0</sub> = 4.5 to 2 l = 2.8	<ul style="list-style-type: none"> <li>• The friction stir process used for composite fabrication in Al based battery outer body.</li> <li>• Corrosion behavior of the body improved due to FSP modification.</li> </ul>
1100-H14 Al alloy and Nickel <sup>122</sup>	Groove filling and covering	The size of Al <sub>3</sub> Ni formed particles below the 1 $\mu\text{m}$	r = 1180 t = 60 p = 6 (multi-pass) d = 25 d <sub>0</sub> = 9.6 to 5 l = 6	<ul style="list-style-type: none"> <li>• Aluminum and Ni particles forms the composites using FSP, and number of passes takes as process parameter to study the uniform distribution effect of particles.</li> </ul>

*(Contd.)*

Table 6 — FSP processed composites with fabrication method and range of parameters (*Contd.*)

Material system	Method of secondary phase introduction	Grain refinement (in $\mu\text{m}$ )	Parameters	Remarks
Al6082 and Mo particle reinforced <sup>123</sup>	Groove filling and covering	The average grain size of obtained sample was 31.66 $\mu\text{m}$	r = 1600 t = 60 p = single d = 18 d <sub>o</sub> = 6 l = 5.8	<ul style="list-style-type: none"> <li>Volume fraction of Mo particles with Al6082 introduced and effect of different volume fraction observed.</li> <li>The mechanical and microstructure properties improved.</li> </ul>
AA 7075 and Multiwall carbon nano tubes (MWCNT), Copper (Cu) and Silicon carbide (SiC) <sup>124</sup>	Hole filling and covering	Base metal mean dia. observed 50-80 $\mu\text{m}$ and particles size ranges in 5-10 $\mu\text{m}$ .	r = 800 t = 60 d = 20 d <sub>o</sub> = 6 to 4 l = 3 Angle = 3°	<ul style="list-style-type: none"> <li>SiC, Cu and MWCNTs were added as filler with AA7075 matrix for composites fabrication. The effect of different filler particles observed and SiC shows better results among three.</li> </ul>
Commercial 1060 aluminium (Al) and Multi-walled CNTs <sup>125</sup>	Groove filling and Covering	-	r = 600, 750, 950 t = 30, 95, 150 p = three pass d = 20 d <sub>o</sub> = 6 to 4 l = 5	<ul style="list-style-type: none"> <li>MWCNTs introduced with aluminum at different rotational and traverse speed. The high energy input forms the coarse grain structure.</li> </ul>
Al5083 and SiC & CNTs particles used as reinforcement <sup>126</sup>	Groove filling and covering	40 to 6 $\mu\text{m}$	r = 1600 t = 20	<ul style="list-style-type: none"> <li>The SiC and CNTs treated before filling with Al5083 matrix. Mechanical and microstructure characteristics improved comparatively</li> </ul>
AA1050 aluminium alloy and Fe <sub>2</sub> O <sub>3</sub> / Powder <sup>127</sup>	Groove filling and covering	Fabricated hybrid composites with Al matrix mean grain ~3 $\mu\text{m}$	r = 1120, 1400 t = 125, 40 p = four d = 10, 18 d <sub>o</sub> = 6, 5 l = 4	<ul style="list-style-type: none"> <li>The aluminium alloy and Fe<sub>2</sub>O<sub>3</sub> particles were introduced using FSP and particles distributed uniformly throughout composites.</li> </ul>
AZ91 magnesium alloy and SiO <sub>2</sub> <sup>128</sup>	Groove filling and covering	140 to 8 $\mu\text{m}$	r = 1250 t = 20, 40, 63 p = 1, 2, 3 d = 18 d <sub>o</sub> = 6 l = 4	<ul style="list-style-type: none"> <li>Mechanical and corrosion properties evaluated on different processing parameters and behaviour of SiO<sub>2</sub> observed.</li> </ul>

Specification for table presented below; r = Rotational speed (rpm); t = Traverse speed (mm/min); p = number of passes; d = Shoulder diameter (mm); d<sub>o</sub> = pin diameter (mm); l = length of pin (mm)

### 3.2 Data driven study on FSP

In the previous section of the article emphasizes the FSP and its associated parameters. This section provides the brief overview of the parameters in quantitative form based on published articles. A brief systematic representation of the parameter has been shown in Fig. 11. For this study rotational speed, traverse speed, shoulder diameter, pin diameter, pin length, tool tilt angle, base materials and reinforcement as parameters taken into consideration from total 536 published article, in which articles are from journals sci

based and Scopus based, international conferences. These published articles are on the experimental basis study and included article from 2011 to 2020. The data from the different article taken on basis of author's findings. The value is taken on which the defect free sample has been fabricated during study. It clearly observable from the Fig. 11, material for the FSP, aluminum have been utilized mostly compare to others like magnesium, titanium and copper. With 76% articles from total 536, are based on aluminum alloys. Advancement in automobile or better to say industries to make the product fuel efficient and weight reduction, works on the aluminum alloys. The weight to strength ratio also an important factor which taken into consideration in designing the product. So, aluminum alloys mostly used in FSP application as base material.

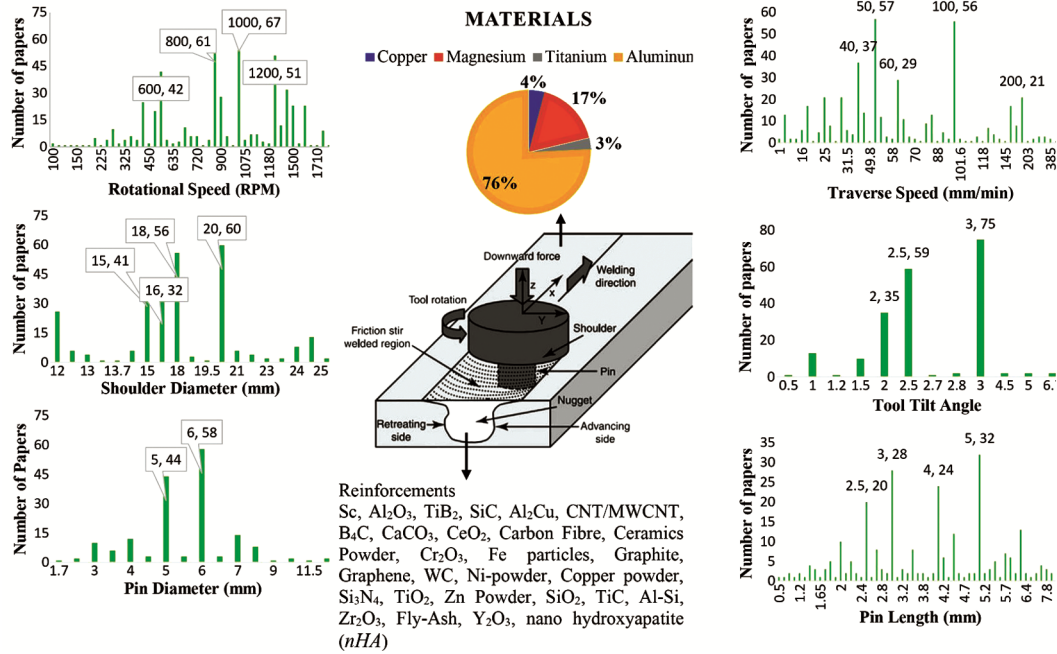


Fig. 11 — Identification of different FSP parameters and materials from published literatures.

For surface composites fabrication secondary phase added to the base material, and processed through FSP. Some of the secondary phase particles used with base material in FSP, has been identified and shown in Fig. 11. Rotational and traverse speed are the power-driven parameters provided directly from rotating motor or electric equipment. So, it is necessary to understand the which values are most important in terms of final product is defect free or objective could be achieved. Several researchers on their studies includes the parameters and for those different values also. The values which give the results according the study considered as most influencing values. Here, for rotational speed parameters the range of values taken into consideration between 100-2500 RPM. The values for rotational speed are most commonly used 600, 800, 1000 and 1200 rpm from published article like 42, 61, 67 and 51 respectively. For the traverse speed the data range is from 1 to 200 mm/min. In which 40, 50, 60 and 100 mm/min have the published paper more compare to other values from range. As discussed earlier for tool tilt angle so its value like 2°, 2.5° and 3° have the mostly used in publication.

Now comes to tool which includes the shoulder and pin, so shoulder to generate heat with most commonly used with 15 mm, 16 mm, 18 mm and 20 mm diameter. Similarly for pin part its diameter and length are important. Which plays for the uniform distribution

and decide the depth of surface composites as well. Stirring effect provided by the pin which decide the flow of the material for fine and equiaxed grain structure. Also, D/d ratio is important for defect free study of FSP based product/surface application. For deciding the pin diameter value 5 mm and 6 mm diameter for pin mostly used. For length 2.5 mm, 3 mm, 4 mm and 5 mm length most commonly used in published article. There is also more parameter which influence the process as well as need to considered. For this study limited to these parameters and upto certain published papers. Basic idea about parameters and its related values has been discussed in this section gives better understanding of FSP.

The correct application of parameters during the procedure resulted in a refined grain structure and FSP application. Fig. 11, shows a quantitative analysis of the many parameters previously addressed. If the parameters are not employed in a controlled manner, faults will appear on the surface<sup>129</sup>. Temperature and metal flow impact FSP flaws, which may be controlled by process factors such tool design, rotational speed, traverse speed, and tool tilt angle<sup>130</sup>. Table 7, shows some of the problems, along with their definitions, reasons, and illustrations. This provides a quick summary of defects as well as the reasons for the related parameters. Defects might be controlled and parameters adjusted by identifying the parameters.

Table 7 — Types of defects in FSP with possible causes

Name	Definition	Cause
Lack of penetration <sup>131</sup>	There is a lack of mechanical and chemical bonding in the groove, and it has not been penetrated to the depth specified.	<ul style="list-style-type: none"> <li>• Inadequate pin tool penetration depth or seam tracking</li> <li>• Workpiece thickness fluctuation</li> </ul>
Wormhole/Void/lack of surface fill <sup>132</sup>	Formation of a hollow on the side that is moving forward	<ul style="list-style-type: none"> <li>• Excessive rotational and traverse speeds are employed, as well as a flat-shouldered tool, due to a lack of heat input and material flow.</li> <li>• Weld pitch is too high.</li> <li>• Forging pressure is insufficient</li> </ul>
Flash defect/Tunnel <sup>133</sup>	Excessive material removal from the workpiece's surface during reverse side processing. AS in the toe corner.	<ul style="list-style-type: none"> <li>• Excessive heat is applied, resulting in excessive axial stress, high rotation speed, and high tool tilt angle.</li> <li>• Inadequate heat input and poor material flow</li> </ul>
Nugget/groove collapse <sup>134</sup>	On the surface, the nugget/pothole form increases insufficiently.	<ul style="list-style-type: none"> <li>• Due to high traversal speed, this happens due to increased heat and material movement into the stir zone.</li> <li>• A tilting angle that is either very little or very large.</li> </ul>
Lack of Fusion <sup>135</sup>	Laps of incomplete fusion	<ul style="list-style-type: none"> <li>• Due to the presence of contaminants on the material's surface and edge.</li> </ul>
Kissing bond/Zigzag defects <sup>136</sup>	Metallic bonding is absent or there is little separation at the interface with the base material.	<ul style="list-style-type: none"> <li>• Insufficient material stirring with lower heat input, higher welding speed and lower rotating speed.</li> </ul>
Surface galling <sup>137</sup>	Metal shredding from the weld surface near the top.	<ul style="list-style-type: none"> <li>• Because of the workpiece material clinging to the tool pin during processing and the fast traverse speed.</li> </ul>
Root Flow Defect	Softening of the workpiece causes it to adhere to the backing plate.	<ul style="list-style-type: none"> <li>• This occurs as a result of excessive pin length and heat causing over penetration.</li> </ul>
Scalloping	In the weld zone, on the advancing side of the weld/processing zone, a series of small voids appear.	<ul style="list-style-type: none"> <li>• Inadequate shoulder and pin diameters cause this.</li> </ul>
Oxide entrapment	When oxygen and aluminium react, an oxide is formed, which entraps the processing zone.	<ul style="list-style-type: none"> <li>• Occurs as a result of improper surface preparation prior to the procedure.</li> </ul>

In Table 7, types of defects have been identified on the basis of process parameters selection. Friction between the tool shoulder and pin with the base material generate the heat. Flow of the plasticized material takes place due to stirring action of the tool. Improper selection of parameters like rotational speed or transversal speed might generate more heat from the required material flow. Flash, tunnel, nugget, groove/surface falling are the defects that occur due to more heat generation. So, this heat generation can be optimized by controlling rotational speed and friction between the tool and workpiece. Lack of heat over the zone also produces defects like wormhole, void, lack of fusion and lack of penetration. The proper implementation of process parameters like rotational speed, traverse speed, coefficient of friction between surfaces resolves the low heat generation. During the FSP, proper forging force is required to maintain the proper flow and uniform distribution of flowing material otherwise it may form wormholes and flash. As discussed earlier, tool profile is also important to achieve defect-free products processed through FSP.

Inadequate selection of tool profile generates root flow defect, scalloping, surface galling and tunnel-like structure over the surface. Sometimes prior processing of processed specimen is required to remove surface oxides or rust otherwise it may react with base material during processing and result in oxide entrapment or foreign particle entrapment. These are the issues that need to be taken into consideration during friction stir process to improve surface quality and defect-free material.

Furthermore, FSP has significant potential in manufacturing processes such as friction stir additive manufacturing, ultrasonic assisted friction stir processing<sup>138</sup>, plasma nitriding<sup>139</sup>, induction assisted process<sup>140</sup>, and others, resulting in significant advances toward the goal of innovative and modern manufacturing engineering applications. For FSP including multiple process factors impacting the process, an approach is also necessary for the formulation and development of mathematical models<sup>141</sup>, optimization techniques<sup>142,143</sup> and artificial intelligence<sup>144</sup>.

#### 4 Conclusion

This article based on the study of Friction stir process, which is emerging to improve surface characteristics of the material. Advancement with the FSP technique has been developed and further research work going on to make it feasible for industrial application. Some of the conclusion has been made which briefly given below

- To make more competitive friction stir process, research has focused on novel material development to decreasing or eliminating casting defects, enhancing process stability, creating components having high mechanical performance and fine quality.
- An in-depth understanding of multiple ideal process parameters, materials, reinforcement, in-process parameter, tool design control is necessary to achieve such a goal. For defect free of material, the most suitable FSP process parameter selection can make sure that process is stable.
- Moreover, reliable and integrated process control and monitoring arrangements are required to conserve the process steadiness and guarantee production eminence. The selection of vertical milling machine with optimised process parameters makes defect free product without any interruption during friction stir process.
- Generally, the heating and flow of the material are considered in control and monitoring process. Through designing the parameters in such a way, the mechanical properties, micro structural evolution and material characteristics can be optimized.
- On material properties, specific influence occurs by different alloying elements. Number of organic and synthetic reinforcement used with base material to improve the surface and wear properties. The use of secondary phase contributes to waste material utilization. The summary of the process parameters working range could identify the limits and reduce the defects occurring by the un-relevant use of parameters.
- The industries like automotive, aerospace, biomedical, nuclear more emphasize the process associated with surface properties enhancement. The friction stir process improved by associating with other technique to make use with industries economically. Because of the highly complex nature of FSP, achieving this significant

milestone, while within the reach of the engineering research community, will necessitate decades of research and development.

#### References

- 1 Pujara Y, Pathak P, Sharma A, & Govani J, *J Environ Manage*, 248 (2019) 109238.
- 2 Jha M K, & Rangarajan K, *Sustain Dev*, 28 (2020) 1019.
- 3 Arora H S, Singh H, & Dhindaw B K, *Int J Adv Manuf Technol*, 61 (2012) 1043.
- 4 Rajendran C, Srinivasan K, Balasubramanian V, Balaji H, & Selvaraj P, *Int J Light Mater Manuf*, 4 (2021) 480.
- 5 Mishra R S, & Ma Z Y, *Mater Sci Eng R Reports*, 50 (2005).
- 6 Sharma R K, Sodhi G P S, Bhakar V, Kaur R, Pallakonda S, Sarkar P, & Singh H, *CIRP J Manuf Sci Technol*, 30 (2020) 25.
- 7 Jain V, Mishra R S, Verma R, & Essadiqi E, *Scr Mater*, 68 (2013) 447.
- 8 Bajakke P A, Malik V R, & Deshpande A S, *Mater Manuf Process*, 34 (2019) 833.
- 9 Rokkala U, Bontha S, Ramesh M R, Balla V K, Srinivasan A, & Kailas S V., *J Mater Res Technol*, 12 (2021) 1530.
- 10 Nithin Joseph Reddy S A, Sathiskumar R, Gokul Kumar K, Soete J, & Vinoth Jebaraj A, *Mater Res Express*, 6 (2019)
- 11 Ajay Kumar P, Madhu H C, Pariyar A, Perugu C S, & Kumar Sharma S, *Mater Sci Eng A*, 769 (2020) 138517.
- 12 Patel S K, Singh V P, Roy B S, & Kuriachen B, *Mater Sci Eng B*, 262 (2020) 114708.
- 13 Balachandran S, Mishra R S, & Banerjee D, *Mater Sci Eng A*, 772 (2020) 138705.
- 14 Guru P R, Khan MD F, Panigrahi S K, & Ram G D J, *J Manuf Process*, 18 (2015) 67.
- 15 Bhojak V, Jain J K, Singhal T S, Saxena K K, Buddhi D, & Prakash C, *Int J Interact Des Manuf*, (2022) 1.
- 16 Ratna Sunil B, Sampath Kumar T S, Chakkingal U, Nandakumar V, & Doble M, *Mater Sci Eng C*, 39 (2014) 315.
- 17 Bheekya Naik R, Venkateswara Reddy K, Madhusudhan Reddy G, & Arockia Kumar R, *Fusion Eng Des*, 164 (2021) 112202.
- 18 Naik R B, Reddy K V, Reddy G M, & Arockia Kumar R, *Mater Lett*, 265 (2020) 127437.
- 19 Mahto M K, Kumar A, Raja A R, Vashista M, & Yusufzai M Z K, *CIRP J Manuf Sci Technol*, 36 (2022) 23.
- 20 Raja A R, Vashista M, & Khan Yusufzai M Z, *J Alloys Compd*, 814 (2020) 152265.
- 21 Parumandla N, & Adepu K, *Mater Sci*, 24 (2018) 338.
- 22 Ramesh K N, Pradeep S, & Pancholi V, *Metall Mater Trans A* 2012, 43 (2012) 4311.
- 23 Kumar K, & Kailas S V, *Mater Sci Eng A*, 485 (2008) 367.
- 24 M Prabhu S, A Perumal E, & Arulvel S, *Surf Coatings Technol*, 394 (2020) 125900.
- 25 Shyam Kumar C N, Yadav D, Bauri R, & Janaki Ram G D, *Mater Sci Eng A*, 645 (2015) 205.
- 26 Sudhakar I, Madhusudhan Reddy G, & Srinivasa Rao K, *Def Technol*, 12 (2016) 25.
- 27 Jain V, Mishra R S, Gupta A K, & Gouthama, *Mater Sci Eng A*, 560 (2013) 500.
- 28 Ali Anshari M A, Imam M, Khan Yusufzai M Z, Chinthapenta V, & Mishra R, *Mater Sci Eng A*, 805 (2021) 140582.

- 29 Joyson Abraham S, Chandra Rao Madane S, Dinaharan I, & John Baruch L, *J Asian Ceram Soc*, 4 (2016) 381.
- 30 Raja A, Biswas P, & Pancholi V, *Mater Sci Eng A*, 725 (2018) 492.
- 31 Yadav D, Bauri R, & Chawake N, *Mater Charact*, 136 (2018) 221.
- 32 Mishra M K, Rao A G, Balasundar I, Kashyap B P, & Prabhu N, *Mater Sci Eng A*, 719 (2018) 82.
- 33 Parumandla N, & Adepu K, *Part Sci Technol*, 38 (2020) 121.
34. Venkateswarlu G, Singh A K, Davidson J, & Tagore G R, *J Mater Res Technol*, 2 (2013) 135.
- 35 Aruri D, Kumar A, & Kotiveerachary B, *Int J Appl Res Mech Eng*, 1 (2020) 152.
- 36 Rao A G, Katkar V A, Gunasekaran G, Deshmukh V P, Prabhu N, & Kashyap B P, *Corros Sci*, 83 (2014) 198.
- 37 Singh S K, Immanuel R J, Babu S, Panigrahi S K, & Janaki Ram G D, *J Mater Process Technol*, 236 (2016) 252.
- 38 Gotawala N, Kumar A, Mishra S, & Shrivastava A, *Mater Today Commun*, 26 (2021) 101850.
- 39 John Baruch L, Raju R, Balasubramanian V, Rao A G, & Dinaharan I, *Acta Metall Sin*, 29 (2016) 431.
- 40 Meenia S, Khan MD F, Babu S, Immanuel R J, Panigrahi S K, & Janaki Ram G D, *Mater Charact*, 113 (2016) 134.
- 41 Das B, Pal S, & Bag S, *Measurement*, 103 (2017) 186.
- 42 Kumar R, Singh K, & Pandey S, *Trans Nonferrous Met Soc China*, 22 (2012) 288.
- 43 Arora K S, Pandey S, Schaper M, & Kumar R, *Int J Adv Manuf Technol*, 50 (2010) 941.
- 44 Sethi D, Acharya U, Shekhar S, & Roy B S, *Def Technol*, (2021)
- 45 Jain R, Pal S K, & Singh S B, *Int J Adv Manuf Technol*, 94 (2017) 1781.
- 46 Jain R, Pal S K, & Singh S B, *J Manuf Process*, 23 (2016) 278.
- 47 Manvatkar V D, Arora A, De A, & DebRoy T, *Sci Technol Weld Join*, 17 (2012) 460.
- 48 Devaraju A, Kumar A, & Kotiveerachari B, *Mater Des*, 45 (2013) 576.
- 49 Kumar H, Vashista M, & Yusufzai M Z K, *Trans Indian Inst Met*, 71 (2018) 2025.
- 50 Kumar H, Khan M Z, & Vashista M, *Mater Res Express*, 5 (2018)
- 51 Sathiskumar R, Dinaharan I, Murugan N, & Vijay S J, *Trans Nonferrous Met Soc China*, 25 (2015) 95.
- 52 Vijayavel P, Ananthakumar K, Rajkumar I, & Sundararajan T, *Met Powder Rep*, xxx (2020) 1.
- 53 Kumar D, & Singh K, *Indian J Eng Mater Sci*, 27 (2020) 58.
- 54 Pradeep S, Sharma S K, & Pancholi V, *Mater Sci Forum*, 710 (2012) 253.
- 55 Nadammal N, Kailas S V, & Suwas S, *Mater Des*, 65 (2015) 127.
- 56 Pradeep S, Sharma S K, & Pancholi V, *Mater Sci Forum*, 702–703 (2012) 348.
- 57 Arora H S, Singh H, Dhindaw B K, & Grewal H S, *Trans Indian Inst Met*, 65 (2012) 735.
- 58 Devanathan C, & Babu A S, *Adv Manuf Autom*, (2013) 482.
- 59 Saini N, Dwivedi D K, Jain P K, & Singh H, *Procedia Eng*, 100 (2015) 1522.
- 60 Malik V, Sanjeev N K, Hebbar H S, & Kailas S V., *Procedia Eng*, 97 (2014) 1060.
- 61 Sadhu A, Patra Karmakar D, Mypati O, Muvvala G, Pal S K, & Nath A K, *Opt Laser Technol*, 128 (2020) 106241.
- 62 Devaraju A, Kumar A, Kumaraswamy A, & Kotiveerachari B, *Mater Des*, 51 (2013) 331.
- 63 Mehdi H, & Mishra R S, *Def Technol*, 17 (2021) 715.
- 64 Madhu H C, Ajay Kumar P, Perugu C S, & Kailas S V., *J Mater Eng Perform*, 27 (2018) 1318.
- 65 Bheekya Naik R, Madhusudhan Reddy G, Kanmani Subbu S, & Arockia Kumar R, *Mater Sci Forum*, 969 (2019) 864.
- 66 Venkateswara Reddy K, Bheekya Naik R, Madhusudhan Reddy G, Chakravarthy P, Janakiram S, & Kumar R A, *Mater Lett*, 298 (2021)
- 67 Pariyar A, Perugu C S, Toth L S, & Kailas S V, *J Alloys Compd*, 880 (2021) 160430.
- 68 Bahl S, Nithilaksh P L, Suwas S, Kailas S V., & Chatterjee K, *J Mater Eng Perform*, 26 (2017) 4206.
- 69 Devaraju A, Kumar A, & Kotiveerachari B, *Trans Nonferrous Met Soc China*, 23 (2013) 1275.
- 70 Kumar A, Pal K, & Mula S, *J Manuf Process*, 30 (2017) 1.
- 71 Bikkina V, Talasila S R, & Adepu K, *Trans Nonferrous Met Soc China*, 30 (2020) 1743.
- 72 Malik V, & Kailas S V., *Proc Inst Mech Eng Part C J Mech Eng Sci*, 235 (2021) 744.
- 73 Gangil N, Maheshwari S, & Siddiquee A N, *Mater Tehnol*, 52 (2018) 77.
- 74 Vijayavel P, & Balasubramanian V, *J Alloys Compd*, 729 (2017) 828.
- 75 Jain R, Pal S K, & Singh S B, *J Eng Manuf*, 233 (2018) 1980.
- 76 Butola R, Pandit D, Pratap C, & Chandra P, *J Adhes Sci Technol*, (2021) 1.
- 77 Thangarasu A, Murugan N, Dinaharan I, & Vijay S J, *Arch Civ Mech Eng*, 15 (2015) 324.
- 78 Butola R, Murtaza Q, & Singari R M, *Indian J Eng Mater Sci*, 27 (2020) 826.
- 79 Zhang Y N, Cao X, Larose S, & Wanjara P, *Can Metall Q*, 51 (2013) 250.
- 80 Meena K, Kumar A, & Pandya S N, *Mater Today Proc*, 4 (2017) 1978.
- 81 Vijayavel P, & Balasubramanian V, *Alexandria Eng J*, 57 (2018) 2939.
- 82 Senthil V, & Balasubramanian E, *Met Powder Rep*, 75 (2020) 110.
- 83 Devanathan C, Boopathi S, Giri R, Shankar E, & Sivanand A, *Mater Today Proc*, 46 (2020) 3169.
- 84 Rana R, Murtaza Q, & Walia R S, *Indian J Eng Mater Sci*, 27 (2020) 889.
- 85 Ramesh Babu S, Pavithran S, Nithin M, & Parameshwaran B, *Procedia Eng*, 97 (2014) 800.
- 86 Vijayavel P, Sundararajan T, Rajkumar I, & Ananthakumar K, *Met Powder Rep*, 76 (2021) 75.
- 87 Cartigueyen S, Sukesh O P, & Mahadevan K, *Procedia Eng*, 97 (2014) 1069.
- 88 Kumar H, Prasad R, Srivastava A, Vashista M, & Khan M Z, *J Clean Prod*, 196 (2018) 460.
- 89 Magibalan S, Senthilkumar P, Senthilkumar C, & Prabu M, *Indian J Eng Mater Sci*, 27 (2020) 458.
- 90 Raja A R, Gupta S K, Vashista M, & Yusufzai M Z K, *Mater Res Express*, 6 (2019) 116108.
- 91 Moona G, Walia R S, Rastogi V, & Sharma R, *Indian J Eng Mater Sci*, 27 (2020) 47.

- 92 Sunil B R, Reddy G P K, Patle H, & Dumpala R, *J Magnes Alloy*, 4 (2016) 52.
- 93 Sharma D K, Badheka V, Patel V, & Upadhyay G, *J Tribol*, 143 (2021)
- 94 Gangil N, Maheshwari S, Siddiquee A N, Abidi M H, El-Meligy M A, & Mohammed J A, *J Mater Res Technol*, 8 (2019) 3733.
- 95 Bharti S, Ghetiya N D, & Patel K M, *Mater Manuf Process*, 36 (2020) 135.
- 96 Rathee S, Maheshwari S, Siddiquee A N, & Srivastava M, *Crit Rev Soild state Mater Sci*, 43 (2017) 334.
- 97 Singh P, & Kandikonda H R, *Indian J Eng Mater Sci*, 28 (2021) 5.
- 98 Banerjee S, Sahoo P, & Davim J P, *Adv Mech Eng*, 13 (2021) 1.
- 99 Kumar H, Prasad R, & Kumar P, *Mater Chem Phys*, 256 (2020) 123720.
- 100 Venkateswara Reddy K, Bheekya Naik R, Rao G R, Madhusudhan Reddy G, & Arockia Kumar R, *Compos Commun*, 20 (2020) 100352.
- 101 Dinaharan I, Saravanakumar S, Kalaiselvan K, & Gopalakrishnan S, *J Asian Ceram Soc*, 5 (2018) 295.
- 102 Bains P S, Sidhu S S, & Payal H S, *Mater Manuf Process*, 31 (2015) 553.
- 103 Naresh P, Kumar A, & Kishore M K, *Mater Sci Forum*, 879 (2017) 1369.
- 104 Singh S, & Chauhan N R, *Indian J Eng Mater Sci*, 28 (2021) 189.
- 105 Aruri D, Kumar A, & Kotiveerachary B, *Int J Mech Ind Eng*, 1 (2020) 10.
- 106 Grewal H S, Arora H S, Singh H, & Agrawal A, *Appl Surf Sci*, 268 (2013) 547.
- 107 Suvarna Raju L, & Kumar A, *Def Technol*, 10 (2014) 375.
- 108 Morisada Y, Fujii H, Nagaoka T, & Fukusumi M, *Mater Sci Eng A*, 419 (2006) 344.
- 109 Lee C J, Huang J C, & Hsieh P J, *Scr Mater*, 54 (2006) 1415.
- 110 Chen T, Zhu Z, Ma Y, Li Y, & Hao Y, *J Wuhan Univ Technol Sci Ed 2010 252*, 25 (2010) 223.
- 111 Asadi P, Givi M K B, & Faraji G, *Materials Manuf Process*, 25 (2012) 1219.
- 112 Asadi P, Faraji G, Masoumi A, & Givi M K B, *Metall Mater Trans A*, 42 (2012) 2820.
- 113 Asadi P, Givi M K B, Rastgoo A, Akbari M, Zakeri V, & Rasouli S, *Int J Adv Manuf Technol*, 63 (2012) 1095.
- 114 Azizieh M, Kokabi A H, & Abachi P, *Mater Des*, 32 (2011) 2034.
- 115 Faraji G, Dastani O, & Akbari Mousavi S A A, *Proc Inst Mech Eng Part B J Eng Manuf*, 225 (2011) 1331.
- 116 Asadi P, Faraji G, & Besharati M K, *Int J Adv Manuf Technol*, 51 (2012) 247.
- 117 Najafi M, Nasiri A M, & Kokabi A H, *Int J Mod Phys B*, 22 (2008) 2879.
- 118 Hanas T, Sampath Kumar T S, Perumal G, Doble M, & Ramakrishna S, *J Mater Process Technol*, 252 (2018) 398.
- 119 Balakrishnan M, Dinaharan I, Palanivel R, & Sivaprakasam R, *J Magnes Alloy*, 3 (2015) 76.
- 120 Ahmadkhaniha D, Heydarzadeh Sohi M, Salehi A, & Tahavvori R, *J Magnes Alloy*, 4 (2016) 314.
- 121 Zheng X, Zhang T, Yang H, Zheng Q, Gao Y, Liu Z, Wang W, & Wang K, *Electrochim Acta*, 354 (2020) 136635.
- 122 Qian J, Li J, Xiong J, Zhang F, & Lin X, *Mater Sci Eng A*, 550 (2012) 279.
- 123 Selvakumar S, Dinaharan I, Palanivel R, & Ganesh Babu B, *Mater Charact*, 125 (2017) 13.
- 124 Deore H A, Mishra J, Rao A G, Mehtani H, & Hiwarkar V D, *Surf Coatings Technol*, 374 (2019) 52.
- 125 Zhang S, Chen G, Wei J, Liu Y, Xie R, Liu Q, Zeng S, Zhang G, & Shi Q, *J Alloys Compd*, 798 (2019) 523.
- 126 Jain V K S, Yazar K U, & Muthukumaran S, *J Alloys Compd*, 798 (2019) 82.
- 127 Azimi-Roeen G, Kashani-Bozorg S F, Nosko M, & Švec P, *Mater Charact*, 127 (2017) 279.
- 128 Khayyamin D, Mostafapour A, & Keshmiri R, *Mater Sci Eng A*, 559 (2013) 217.
- 129 Rajeswari S, & Sivasakthivel P S, *Indian J Eng Mater Sci*, 27 (2020) 590.
- 130 Kumar A, Gotawala N, Mishra S, & Shrivastava A, *CIRP J Manuf Sci Technol*, 32 (2021) 170.
- 131 Sivanesh Prabhu M, Elaya Perumal A, Arulvel S, & Franklin Issac R, *Meas J Int Meas Confed*, 142 (2019) 10.
- 132 Kumaraswamy S, Malik V, Devaraj S, Jain V K, & Avinash L, *Mater Today Proc*, 45 (2020) 299.
- 133 Singh S, & Pal K, *Ceram Int*, 47 (2021) 14809.
- 134 Dixit S, Mahata A, Mahapatra D R, Kailas S V., & Chattopadhyay K, *Compos Part B Eng*, 136 (2018) 63.
- 135 Rana H, & Badheka V, *J Mater Process Technol*, 255 (2018) 795.
- 136 Sharma S K, & Pancholi V, (2010) 1.
- 137 Kumar K, Kailas S V, & Srivatsan T S, *Mater Manuf Process*, 26 (2011) 915.
- 138 Sonia P, Jain J K, & Saxena K K, *Adv Mater Process Technol*, 36 (2021) 1451.
- 139 Rathee S, Maheshwari S, & Siddiquee A N, *Mater Manuf Process*, 33 (2018) 239.
- 140 Mohan D G, & Gopi S, *Aust J Mech Eng*, 18 (2018) 119.
- 141 Prudhvi Sai P, Roshan Balu T M B, Vaira Vignesh R, Bhaskara Sastry C V, & Padmanaban R, *Mater Today Proc*, 46 (2021) 7215.
- 142 Singh S, Singh R, & Gill S S, *Indian J Eng Mater Sci*, 27 (2020) 481.
- 143 Bhojak V, Lade J, Jain J K, Patnaik A, & Saxena K K, *Adv Mater Process Technol*, (2022) 1.
- 144 Chintalu R S, Padmanaban R, & Vignesh R V, *Mater Today Proc*, 46 (2021) 7452.